THE JOURNAL OF BIOLOGICAL CHEMISTRY VOL. 289, NO. 8, pp. 4735–4742, February 21, 2014

Conopeptide Vt3.1 Preferentially Inhibits BK Potassium Channels Containing β4 Subunits via Electrostatic Interactions*

Received for publication, November 17, 2013, and in revised form, December 27, 2013 Published, JBC Papers in Press, January 7, 2014, DOI 10.1074/jbc.M113.535898

Min Li[‡§], Shan Chang[¶], Longjin Yang[‡], Jingyi Shi[§], Kelli McFarland[§], Xiao Yang[§], Alyssa Moller[§], Chunguang Wang[‡], Xiaoqin Zou[¶], Chengwu Chi[‡‖1], and Jianmin Cui[§2]**

*From the [‡]Institute of Protein Research, Tongji University, Shanghai 200092, China, the [§]Department of Biomedical Engineering, Washington University, St. Louis, Missouri 63130, the [¶]Department of Physics and Astronomy, Department of Biochemistry, Dalton Cardiovascular Research Center, and Informatics Institute, University of Missouri, Columbia, Missouri 65211, the [‖]State Key Laboratory of Molecular Biology, Institute of Biochemistry and Cell Biology, Shanghai Institutes for Biological Sciences, The Chinese Academy of Sciences, Shanghai 200031, China, and the **Department of Pharmacology, Soochow University College of Pharmaceutical Sciences, Suzhou 215123, China*

Background: BK channel function is differentially modulated by tissue-specific β (β1–4) subunits.
Results: Conopeptide Vt3.1 preferentially inhibits neuronal BK channels containing the β4 subunit.
Conclusion: Electrostatic interactions between Vt3.1 and the extracellular loop of β4 decrease voltage-dependent activation of the channel.
Significance: Vt3.1 is an excellent tool for studying the structure, function, and roles in neurophysiology of BK channels.

BK channel β subunits (β1–β4) modulate the function of channels formed by slo1 subunits to produce tissue-specific phenotypes. The molecular mechanism of how the homologous β subunits differentially alter BK channel functions and the role of different BK channel functions in various physiologic processes remain unclear. By studying channels expressed in *Xenopus laevis* oocytes, we show a novel disulfide-cross-linked dimer conopeptide, Vt3.1 that preferentially inhibits BK channels containing the β4 subunit, which is most abundantly expressed in brain and important for neuronal functions. Vt3.1 inhibits the currents by a maximum of 71%, shifts the *G-V* relation by 45 mV approximately half-saturation concentrations, and alters both open and closed time of single channel activities, indicating that the toxin alters voltage dependence of the channel. Vt3.1 contains basic residues and inhibits voltage-dependent activation by electrostatic interactions with acidic residues in the extracellular loops of the slo1 and β4 subunits. These results suggest a large interaction surface between the slo1 subunit of BK channels and the β4 subunit, providing structural insight into the molecular interactions between slo1 and β4 subunits. The results also suggest that Vt3.1 is an excellent tool for studying β subunit modulation of BK channels and for understanding the physiological roles of BK channels in neurophysiology.

Large conductance, voltage, and Ca^{2+}-activated K^+ (BK) channels regulate neuronal excitability (1, 2), neurotransmission (3), and circadian rhythm (4). BK channels are also important for physiological processes other than in the nervous system such as smooth muscle contraction (5). BK channels are formed by a tetramer of slo1 α subunits that contain the voltage sensor, Ca^{2+}-binding sites, and the pore (6). Four auxiliary β subunits, β1–β4, which are distributed in a tissue-specific manner, modulate functional properties of the channel, thereby providing a major mechanism for tissue-specific phenotypes of BK channels (7–9). The β4 subunit is predominantly expressed in brain where it is more abundant than any other β subunits (9, 10). Therefore, the BK channels comprised of slo1 + β4 are considered as the neuronal type. Although the association of β4 subunits is important for BK channel function, the molecular mechanism of how various β subunits modulate specific characteristics of channel function and the role of these channels in different physiological processes are still not clear.

Marine predatory cone snails produce conotoxins and conopeptides to stun and paralyze animals for prey capturing and defense. The conotoxins and conopeptides modulate the function of ion channels, transporters, and surface receptors in nervous and muscular systems for fast action to enable the slow moving cone snails against their agile opponents (11). Conotoxins or conopeptides are short peptides consisting of 10–40 amino acid residues. They are classified by the "superfamilies" according to highly conserved signal sequences in the precursors as well as "families" based on different characteristic cysteine arrangements and different targets (12). Generally, there are two or more disulfide bonds in conotoxins, but only one or no disulfide bonds could be found in conopeptides (12). Among venom peptide families ω-, μ-, μO-, δ-, ι-, and κ-conotoxins have been demonstrated to interact with voltage-gated Ca^{2+}, Na^+, and K^+ channels (11, 13). These peptide toxins have been valuable tools in studying the structure-function relations and

* This work was supported, in whole or in part, by National Institutes of Health Grants R01-HL70393 and R01-NS060706. This work was also supported by Chinese Ministry of Science and Technology Grant 2010CB529802 (to M. L.), National Science Foundation of China Grant 31271143 (to J. C.), and National Science Foundation Career Award Grant DBI-0953839 (to X. Z.).
[1] To whom correspondence may be addressed: Inst. of Protein Research, Tongji University, 1239 Siping Rd., Shanghai 200092, China. Tel.: 86-21-54921165; E-mail: zwqi@sibs.ac.cn.
[2] To whom correspondence may be addressed: Dept. of Biomedical Engineering, Washington University, 290C Whitaker Hall, One Brookings Dr., St. Louis, MO 63130. Tel.: 314-935-8896; Fax: 314-935-7448; E-mail: jcui@wustl.edu.

physiological roles of ion channels. A number of ion channel targeting conotoxins have also been used to diagnose ion channel-associated diseases and as drug candidates to affect important biological processes (13). Among these conotoxins, the ω-conotoxin MVIIA targets on the N-type Ca^{2+} channels that are related to algesia in the nervous system (14). Based on MVIIA, the synthetic peptide named ziconotide became the first cone snail-derived drug approved by the United States Food and Drug Administration in use for the treatment of severe chronic pain (15, 16).

Vt3.1 was identified from *Conus vitulinus* by cDNA cloning using the M superfamily signal sequence (17). However, unlike other M superfamily conotoxins, Vt3.1 represents a novel group of conopeptides, being a disulfide-cross-linked dimer with an unusual amino acid sequence (see Fig. 1*A*). After *in vitro* refolding of the Vt3.1 peptide, two distinct fractions, Vt3.1 (with cross-disulfides) and Vt3.2 (with parallel disulfides) could be purified. Mice showed hyperactivities upon 20 μg of Vt3.1 by intraventricular injection. On the other hand, Vt3.2 at the same dose of injection did not cause behavioral abnormality in mice (17). We have screened several conopeptides on their modulation of BK channel function and found that Vt3.1 preferentially inhibited the channel comprised of mslo1 + β4 by altering voltage-dependent activation via electrostatic interactions with the channel protein. Using Vt3.1 as a unique probe, these studies showed that the extracellular loop of the β4 subunit is important for modulating BK channel voltage-dependent gating and revealed structural features of slo1-β4 interaction.

EXPERIMENTAL PROCEDURES

Chemical Synthesis and in Vitro Refolding of Vt3.1—The linear Vt3.1 peptide and all of its mutants were synthesized chemically, refolded *in vitro*, and purified as previously described (17).

Oocyte Harvesting and mRNA Injection—Stage IV–V oocytes from female *Xenopus laevis* were harvested and digested by collagenase type 1A (Sigma-Aldrich) following previously described procedures (18). Each oocyte was injected with 0.05–20 ng of mslo1 mRNA or a mixture of mslo1 and β subunit (as 1: 4 ratio) mRNAs and then incubated in ND96 solution (96 mM NaCl, 2 mM KCl, 1.8 mM $CaCl_2$, 1 mM $MgCl_2$, 5 mM Hepes, pH 7.6) at 18 °C for 2–4 days before recording.

The mbr5 splice variant of mslo1 (19), human β1 (KCNMB1, GenBank™ accession number U25138), β2 (KCNMB2, GenBank™ accession number AF209747), β3b, (KCNMB3, GenBank™ accession number AF214561), and β4 (KNCMB4, GenBank™ accession number AF207992) were used. The β2 with N-terminal residues 2–20 deleted (β2ND) was studied to remove inactivation (18). Chimeras between the β1 and β4 subunits were made as follows: C1-4-1, amino acids Pro^{40}–Gln^{155} of β1 were replaced by amino acids Ser^{41}–Ile^{168} of β4; C4-1-4, amino acids Ser^{41}–Ile^{168} of β4 were replaced by amino acids Pro^{40}–Gln^{155} of β1. All mutants were made using overlap extension PCR (20) and verified by sequencing.

Electrophysiology—Macroscopic and single channel currents were recorded from outside-out patches formed with borosilicate pipettes with 1.0–3.5 MΩ resistance. The data were acquired using an Axopatch 200-B patch-clamp amplifier (Axon Instruments, Union City, CA) and Pulse acquisition software (HEKA Electronik, Lambrecht/Pfalz, Germany). Recordings were digitized at 20-μs intervals and low pass filtered at 10 kHz with the 4-pole Bessel filter built in the amplifier. Capacitive transients and leak currents were subtracted using a P/5 protocol. Experiments were performed at room temperature (20–22 °C). The external solution contained 140 mM $KMeSO_3$, 20 mM Hepes, 2 mM KCl, and 2 mM $MgCl_2$, pH 7.2. The internal (pipette) solution contained 140 mM $KMeSO_3$, 20 mM Hepes, 2 mM KCl, and 1 mM HEDTA,[3] pH 7.2. $[Ca^{2+}]_i$ was 10 μM unless indicated otherwise. $CaCl_2$ was added to the internal solution to give the appropriate free $[Ca^{2+}]_i$, which was measured with a calcium-sensitive electrode (Orion Research, Cambridge, MA). 18-Crown-6-tetracarboxylic acid (50 μM; Sigma-Aldrich) was added to internal solutions to chelate Ba^{2+}. For nominal $[Ca^{2+}]_i$, the same internal solution was used except that HEDTA was replaced by 5 mM EGTA and no $CaCl_2$ was added, and the free $[Ca^{2+}]_i$ was 0.5 nM. The duration of single channel open and closed states was analyzed using Qub (State University of New York, Buffalo, NY), and channel open probability was fitted using clampfit 9 (Axon Instruments, Inc., Union City, CA). For macroscopic currents, *G-V* relations were measured from the tail currents and fitted with the following Boltzmann equation,

$$G/G_{max} = 1/(1 + \exp(-(V - V_{1/2})/S)) \quad \text{(Eq. 1)}$$

where *G* is conductance, $V_{½}$ is the voltage at which the channels are half-activated, and *S* is the slope factor. Igor Pro (WaveMetrics, Inc., Lake Oswego, OR) was used for curve fittings.

Toxin Vt3.1 and Vt3.2 were dissolved in the extracellular solution at 1 mM as stock, and aliquots were stored in −80 °C and diluted to the indicated concentrations (see Figs. 1–6) before experiment. The dose-response curve in Fig. 2*B* was fitted to the following equation,

$$I/I_0 = 1 - (1 - A)(1/(1 + K/[T])) \quad \text{(Eq. 2)}$$

where I/I_0 is the ratio of current after and before Vt3.1 application, *A* is the fraction of the remaining current at saturating amounts of Vt3.1, [T] is Vt3.1 concentration, and *K* is the concentration of Vt3.1 for half-maximum inhibition.

Model of Vt3.1—The structure of a monomeric Vt3.1 peptide was generated by using PEP-FOLD, a *de novo* structure prediction server (21), which was then optimized by long time scale molecular dynamics simulations using the NAMD program (version 2.9) (22).

Specifically, the CHARMM 27 all-atom force field (49) was used. During each simulation, the protein was solvated in a cubic periodic box of TIP3P water molecules that extended 10 Å from the protein. Each simulation consisted of two preparation steps. First, the system was minimized by 10,000 steps of energy minimization. Second, the system was slowly heated up from 0 to 298 K over a period of 0.5 ns with a harmonic constraint of 1 kcal·mol^{-1}· Å^{-2} placed on all backbone atoms. Then, non-constrained MD stimulations were performed at constant pressure (1 atm) and constant temperature (298 K) for

[3] The abbreviations used are: HEDTA, *N*-(2-hydroxyethyl)ethylenediamine-*N*,*N*,*N*-triacetic acid; ChTx, charybdotoxin; IbTx, iberiotoxin.

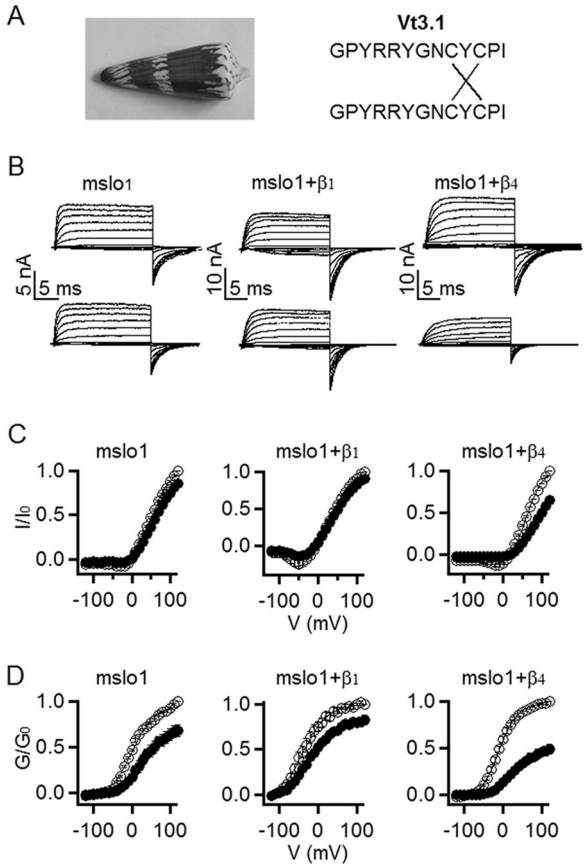

FIGURE 1. **Vt3.1 preferentially inhibits mslo1 + β4 subunit.** *A*, Vt3.1 comes from *Conus vitulinus*, formed by a peptide dimer with two cross-disulfide bonds. *B*, currents in the absence (*top row*) and presence (*bottom row*) of Vt3.1. Testing voltage pulses were −200 to +120 mV with +20 mV increments. Holding potential was −80 mV; repolarization potential was −80 (mslo1) or −120 mV (mslo1 + β1, mslo1 + β4). *C*, normalized peak currents *versus* voltage (*I-V*) relationship in the absence (*open circles*) and presence (*filled circles*) of 10 μM Vt3.1. Currents were normalized to the largest current before Vt3.1 application. *D*, *G-V* relationship in the absence (*open circles*) and presence (*filled circles*) of 10 μM Vt3.1. Tail currents at the repolarization were normalized to the largest current before Vt3.1 application. Smooth curves are Boltzmann equation (Equation 1) fits to the mslo1 data with $V_{1/2}$ values of 0.54 ± 0.89 and 25.3 ± 3.6 mV (S.E.) and slope factor (*S*) values of 29.4 ± 2.7 and 30.8 ± 3.7 (S.E.) in the absence and presence of Vt3.1 ($n = 6$); for mslo1 + β1, $V_{1/2}$ values are −45.1 ± 3.1 and −29.7 ± 1.9 mV (S.E.), and slope factor (*S*) values are 25.8 ± 0.9 and 30.5 ± 0.82 (S.E.) in the absence and presence of Vt3.1 ($n = 7$); for mslo1 + β4, $V_{1/2}$ values are −15.0 ± 2.6 and 30.4 ± 4.5 mV (S.E.), and slope factor (*S*) values are 20.6 ± 1.1 and 26.7 ± 0.94 (S.E.) in the absence and presence of Vt3.1, respectively ($n = 8$). The normalized amplitudes for mslo1, mslo1 + β1, and mslo1 + β4 with the toxin presence are 68.1 ± 6.7, 82.6 ± 4.7, and 48.9 ± 3.8% compared with controls.

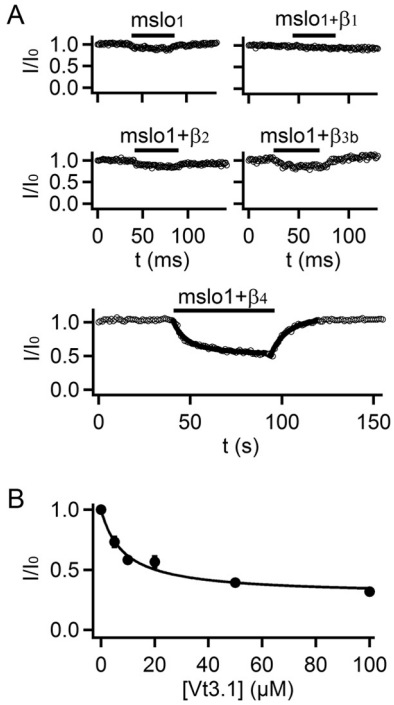

FIGURE 2. **Vt3.1 preferentially inhibits mslo1 + β4 subunit.** *A*, time course of Vt3.1 inhibition. Double- and single-exponential functions were fitted to the onset and washout of Vt3.1 effects on mslo1 + β4 (*thick solid line*), respectively ($n = 8$). *B*, response of peak currents to toxin doses for mslo1 + β4. The smooth curve is fitting to Equation 2 with $K = 8.5$, $A = 0.29$ ($n = 4$).

80 ns. The SHAKE algorithm (50) was applied for bond constraints, and the particle mesh Ewald (PME) method (51) was used to calculate electrostatic interactions. A cutoff of 1.2 nm was used for the Lennard-Jones interactions. For each simulated system, the trajectory snapshots were saved every 2.0 ps; a total of 40,000 conformations were collected for further analysis.

RESULTS

Vt3.1 Preferentially Inhibits BK Channels Containing the β4 Subunit—During the screen of peptide conotoxins against BK channels, we found that Vt3.1 (Fig. 1*A*) inhibits channels formed by the mslo1 subunit; the maximal conductance in the presence of toxin is smaller than that of control (Fig. 1, *B* and *C*). To examine whether any β subunit can alter the toxin inhibition, we measured the effect of 10 μM Vt3.1 on the currents from coexpression of mslo1 with the β1, β2, β3b, and β4 subunit, respectively. The toxin inhibition was slightly reduced by the coexpression of the β1 subunit, but not altered by the β2 or β3b subunits; on the other hand, the β4 subunit enhanced the inhibition by more than 2-fold (Figs. 1, *C* and *D*, and 2*A*). The toxin inhibition showed a weak voltage dependence. At −120 mV, the tail current corresponding to the maximal conductance elicited by a +80 mV test pulse was reduced by 58.8 ± 4.8% for mslo1 + β4 (Fig. 1, *B* and *D*), whereas the current at the +80 mV test pulse *per se* was reduced by 34.3 ± 2.8% (Fig. 1, *B* and *C*). Similar to mslo1, the mslo1 + β4 channels respond to Vt3.1 quickly, with a fast inhibition time constant of 6.4 ± 1.7 s and then followed with a slower current decrease of a time constant ≥20.2 ± 5.7 s. The effect of Vt3.1 can be readily washed out, with a time constant of 7.4 ± 0.6 s (Fig. 2*A*). Vt3.1 did not completely inhibit the currents even with the concentration ([Vt3.1]) up to 100 μM. The inhibition of the mslo1 + β4 by [Vt3.1] can be fitted by a dose-response curve with the maximal inhibition of 71% and the [Vt3.1] at half-inhibition (IC_{50}) of 8.5 μM (Fig. 2*B*).

Vt3.1 Inhibits Voltage-dependent Gating of BK Channels—The results in Fig. 1*D* and 2*B* suggest that the toxin may not inhibit BK channels by directly blocking the pore, but instead by affecting the gating mechanism of the channel. In the presence of Vt3.1, the *G-V* relation is shifted to more positive voltages (also see Fig. 3*C*), whereas the maximum conductance is reduced (Fig. 1*D*). However, even at the saturation of Vt3.1 binding, the channel activity is not completely inhibited, allow-

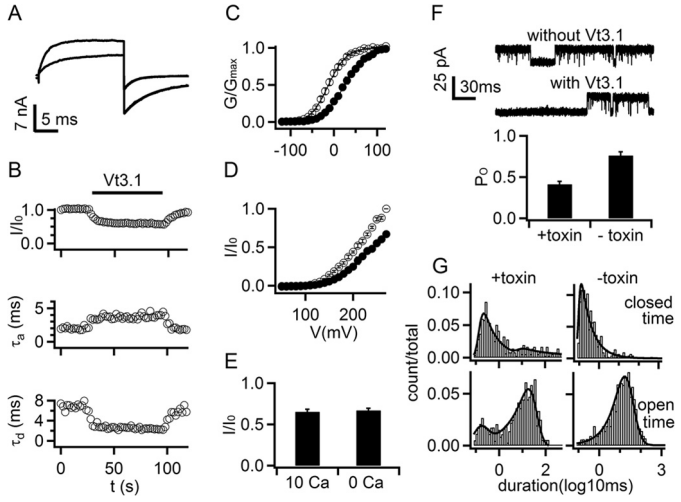

FIGURE 3. **Vt3.1 inhibits voltage-dependent activation of mslo1 + β4.** *A*, current traces before (*gray*) and after (*black*) 10 μM Vt3.1 application. Voltages were: test +80 mV, holding −80 mV, and repolarization −120 mV. Activation and deactivation time courses were fitted with exponential equation (smooth curves superimposed with currents). *B*, changes in current amplitude, activation (τ_a), and deactivation (τ_d) time constants during Vt3.1 application ($n = 7$). *C*, conductance-voltage (*G-V*) relationship in the absence (*open circles*) and presence (*filled circles*) of Vt3.1. Smooth curves are Boltzmann equation (Equation 1) fits to the data with $V_{1/2}$ values of −16.2 ± 2.5 mV and 29.3 ± 3.8 mV (S.E.), and slope factor (*S*) values of 18.6 ± 0.4 and 24.0 ± 0.7 (S.E.) in the absence and presence of Vt3.1, respectively ($n = 8$). *D*, normalized *I-V* relationship in 0 $[Ca^{2+}]_i$ ($n = 9$). *E*, ratio of current amplitude in the presence (*I*) and absence (I_0) of Vt3.1. Currents were measured at voltages where the open probability of the channels were maximal, +100 mV (in 10 μM $[Ca^{2+}]_i$) and +270 mV (in 0 $[Ca^{2+}]_i$). *F*, single channel currents at +80 mV (*upper panel*, open state at *top*) and open probability (*bottom panel*) with and without 10 μM Vt3.1. *G*, single channel dwell time histograms of closed (*top panel*) and open (*bottom panel*) events. In the absence of Vt3.1 (*-toxin*), both open and closed times are fitted by a single exponential with time constant of 16.6 and 0.13 ms, respectively. In the presence of Vt3.1 (+toxin), open time is fitted with two exponentials, one with a time constant of 14.1 ms, similar to that in the absence of Vt3.1, and the other with a shorter time constant of 0.10 ms; close time is fitted with an exponential with a time constant of 0.12 ms, similar to that in the absence of Vt3.1, and with additional longer time constant of 14.4 ms.

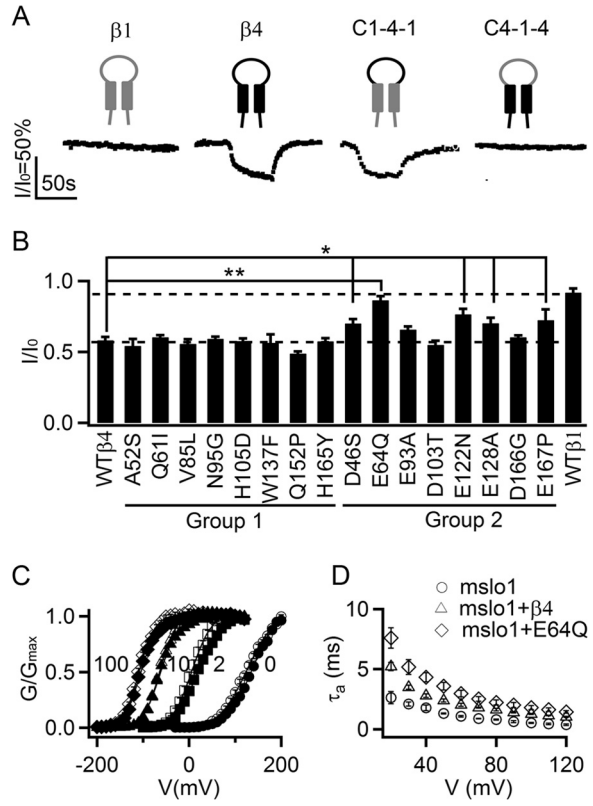

FIGURE 4. **Acidic residues in the extracellular loop of β4 important for Vt3.1 inhibition.** *A*, response of the channels containing chimeras between β1 (*gray cartoon*) and β4 (*black*) to 10 μM Vt3.1. C1-4-1 contained the extracellular loop of β4 and the flanking N and C termini of β1, and C4-1-4 was just the opposite ($n = 6$, each). *B*, mutations of β4 on Vt3.1 inhibition of the channel. Groups 1 and 2 are described in the text. * and **, comparing to WT β4, $p < 0.05$ and 0.001, respectively, analysis of variance least significant difference (LSD) post hoc test ($n = 6$). *C*, *G-V* relations of mslo1 + β4 (*open symbols*, $n = 11$) and mslo1 + E64Q β4 (*filled symbols*, $n = 7$) in 0, 2, 10, and 100 μM $[Ca^{2+}]_i$. *D*, activation time constants for mslo1 ($n = 6$), mslo1 + β4 ($n = 8$), and mslo1 + E64Q β4 ($n = 6$).

ing the pass of ionic currents (Fig. 2*B*). Consistent with this mechanism, in the presence of Vt3.1, the channels that remained open showed an altered voltage-dependent activation, with a slower activation and a faster deactivation time course (Fig. 3*A*). The changes in activation and deactivation kinetics developed in time alongside the onset and washout of the Vt3.1 inhibition of currents (Fig. 3*B*). Normalized conductance-voltage (*G-V*) relations of the channel shifted to more positive voltages by 45.5 mV in the presence of 10 μM Vt3.1 (IC_{50} = ~8.5 μM; Fig. 2*B*) (Fig. 3*C*). All these results indicate that the toxin alters voltage-dependent transitions among the kinetic states during voltage-dependent activation such that the forward activation rate is reduced, whereas the backward deactivation rate accelerated to result in a lower steady state open probability. Fig. 3*D* shows the change of voltage-dependent activation caused by Vt3.1 in the absence of intracellular Ca^{2+}, similar to the toxin effects with the presence of 10 μM $[Ca^{2+}]_i$ (Figs. 1*C* and 3*E*). These results suggest that Vt3.1, applied in the extracellular solution, does not influence the dependence of channel activation on the intracellular Ca^{2+}. Single channel recordings showed that Vt3.1 did not lower the single channel conductance (136 ± 3 *versus* 127 ± 5 pS, +toxin *versus* control) but reduced open probability of the channel (0.41 ± 0.03 *versus* 0.76 ± 0.04, +toxin *versus* control) (Fig. 3*F*) by inducing an open state of shorter lifetime and a closed state of longer lifetime (Fig. 3*G*). Taken together, these results suggest that Vt3.1 inhibits BK channels by altering voltage-dependent gating mechanisms.

Vt3.1 Inhibits BK Channels via Electrostatic Interactions with Slo1 and β4—The β subunits of BK channels share a common membrane topology, with two membrane-spanning segments, short cytoplasmic N and C termini and a long extracellular loop (Fig. 4*A*). To investigate the molecular basis for the ability of the β4 subunit to enhance Vt3.1 inhibition, we made chimeras between the β1 and β4 subunits by switching the extracellular loop and then coexpressed each with mslo1. Vt3.1 inhibition of the channel was enhanced as long as the coexpressed β subunit contained the extracellular loop of β4 (Fig. 4*A*), indicating that the amino acids in the extracellular loop of β4 that are not conserved in β1 are important for the channel protein to interact with Vt3.1. Sequence alignment of the extracellular loop in β subunits reveals the residues that are conserved among β1, β2, and β3b but different in β4. We mutated each of these residues in β4 to the corresponding residues in β1 but found that these mutations did not alter the ability of the β4 subunit to

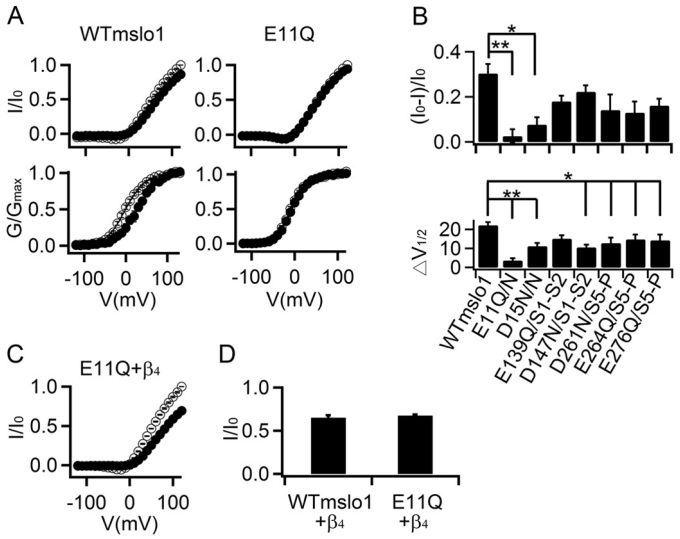

FIGURE 5. **Acidic residues in the extracellular loops of mslo1 important for Vt3.1 inhibition.** *A*, normalized I-V (*top*) and *G-V* (*bottom*) relationships for WT ($n = 6$) and E11Q mslo1 ($n = 11$) without (*open circles*) and with (*filled circles*) 10 μM Vt3.1. *B*, the effects of Vt3.1 on current amplitude at +80 mV (*top panel*) and *G-V* shift (*bottom panel*, $V_{1/2}$ is the voltage where *G-V* relation is at half-maximum) for WT and mutant mslo1 channels. *N*, N terminus; *S1-S2*: the linker between the S1 and S2 transmembrane segment; *S5-P*, the linker between the S5 transmembrane segment and the pore helix. * and **, see Fig. 4 ($n = 12$). *C*, normalized *I-V* of E11Q mslo1 + β4 without (*open circles*) and with (*filled circles*) 10 μM Vt3.1 ($n = 6$). *D*, the effects of Vt3.1 on current amplitude at +100 mV for WT and E11Q mslo1 + β4.

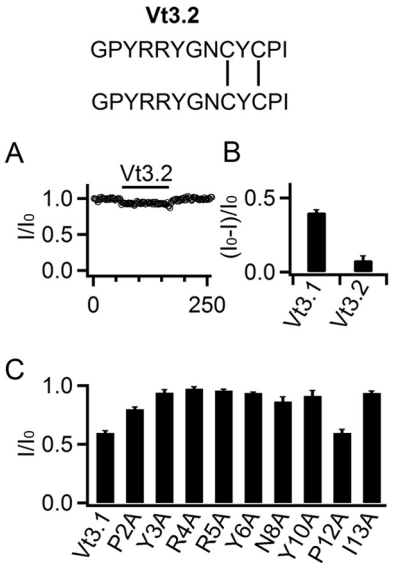

FIGURE 6. **The structure of Vt3.1 is important for channel inhibition.** *A*, response of mslo1 + β4 current amplitude at +80 mV to 10 μM Vt3.2 (structure at top) ($n = 10$). *B*, fraction of mslo1 + β4 currents inhibited by Vt3.1 toxins. *C*, the effects of WT and mutant Vt3.1 on current amplitude ($n = 8$).

enhance Vt3.1 inhibition (Fig. 4*B*, *Group 1* mutations). This finding indicates that these residues are not critical in the interaction with Vt3.1. Next we mutated each of the negatively charged residues in β4 that are not conserved among β1, β2, or β3b (Fig. 4*B*, *Group 2* mutations) to examine possible interactions of these residues with the positive charges on Vt3.1 (Fig. 1*A*). Coexpression of these β mutants with mslo1 showed that a number of the mutations reduced the ability of the β4 subunit to enhance Vt3.1 inhibition, resulting in a phenotype more similar to that of the β1 subunit (Fig. 4*B*). These mutations did not alter the effects of the β4 subunit on BK channel gating. For instance, while reducing the Vt3.1 inhibition by the largest extent, the E64Q mutation did not change the *G-V* relations of mslo1 + β4 (Fig. 4*C*), whereas the E64Q β4 prolonged the time course of BK channel activation similarly to the wt β4 (Fig. 4*D*) (9). These results suggest that the mutation of the negatively charged residues specifically disrupted the interaction between the channel protein and Vt3.1.

The results in Fig. 4 suggest that the negatively charged residues in the β4 subunit extracellular loop enhance the interaction between the channel protein and Vt3.1, leading to an increased Vt3.1 inhibition. To examine whether Vt3.1 also interacts with the negatively charged amino acids in mslo1 channels, we neutralized each of the acidic residues in the extracellular domain of mslo1 by mutation. Glutamic acid 11 is located in the extracellular N terminus of mslo1, and the mutation E11Q eliminated the response of mslo1 to Vt3.1 such that the maximal conductance or the *G-V* relation changed little in the presence of 10 μM Vt3.1 (Fig. 5, *A* and *B*). Neutralization of other negatively charged residues also reduced Vt3.1 inhibition of the mslo1 channel (Fig. 5*B*), suggesting that Vt3.1 interacts with negatively charged residues in the BK channel protein in either the presence or the absence of the β4 subunit to inhibit voltage-dependent activation of the channel. The coexpression E11Q mslo1 + β4 could be inhibited by Vt3.1 (Fig. 5, *C* and *D*), indicating that the interaction of Vt3.1 with β4 is not affected by the disruption of the interaction of Vt3.1 with mslo1. These results suggest that the β4 subunit provides additional interactions with Vt3.1 through negatively charged residues in the extracellular loop to enhance the toxin inhibition of the channel; these negatively charged residues are located throughout the extracellular loop of the β4 subunit and may be close to the negative charges in the extracellular loops of slo1 such that the charges in both slo1 and β4 can interact with Vt3.1, suggesting a large interaction surface between the slo1 subunit of BK channels and the β4 subunit at the extracellular domains (see below).

Structure of Vt3.1 Is Important for Its Inhibition of BK Channels—Vt3.1 is a dimer of two identical Vt3.1 peptides connected via two cross-formed disulfide bonds, *i.e.*, the disulfide bonds formed between Cys^9 of one peptide and Cys^{11} of the other peptide (Fig. 1*A*). The same two peptides can form a different transient dimer, Vt3.2, via two parallel disulfide bonds, *i.e.*, the disulfide bond formed between Cys^9 of each peptide and the disulfide bond formed between Cys^{11} of each peptide (Fig. 6*A*) (17). Unlike Vt3.1, Vt3.2 at 10 μM was unable to inhibit mslo1 + β4 (Fig. 6, *A* and *B*). To examine whether the two pairs of charged residues in Vt3.1, Arg^4 and Arg^5, are critical for the interaction between Vt3.1 and the channel protein, we mutated each to Ala. The mutant toxin could no longer inhibit the channel (Fig. 6*C*). However, we later found that Ala mutation of most of other toxin residues also abolished the ability of Vt3.1 to inhibit the channel (Fig. 6*C*). These results suggest that Vt3.1 may adopt a conformation that is required for its ability to inhibit mslo1 + β4; the different disulfide bond formation in Vt3.2 or mutations in the toxin peptide may disrupt the conformation, leading to the loss of toxin function.

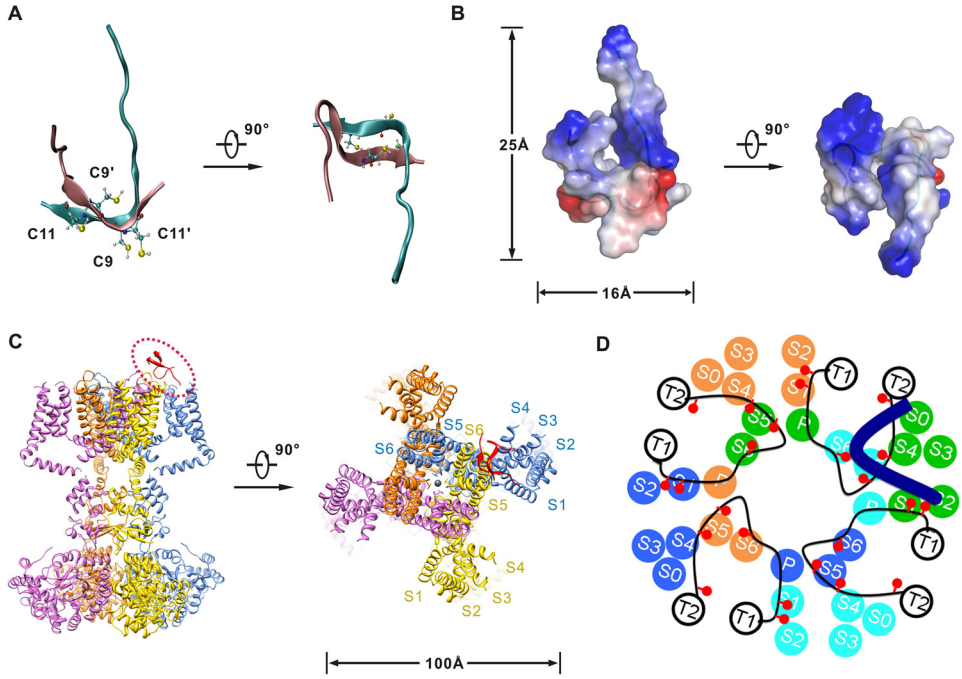

FIGURE 7. **Model of Vt3.1 and its interaction with mslo1 + β4.** *A* and *B*, a representative structure of the Vt3.1 dimer in the stable state after the molecular dynamics simulation. *A*, ribbon diagram. The two chains are colored in *cyan* and *pink*, respectively; the four cysteine residues are shown in ball and stick representation. *B*, surface electrostatic potentials calculated for Vt3.1, positive potentials are shown in *blue*, and negative potentials are in *red*. The two flexible N termini locate on the same side and form a positively charged and flexible domain. *C*, the model structure of Vt3.1 is drawn upon the crystal structure of Kv1.2. *D*, model of Vt3.1 interaction with mslo1 + β4, viewed from the extracellular side into the membrane. Transmembrane segments S0–S6 and the pore helix P for four mslo1 subunits (each color represents one subunit), transmembrane segments T1 and T2 as well as the extracellular loop (*black lines*) of four β4 subunits, and one Vt3.1 molecule (*thick blue line*) are shown. The *red circles* represent acidic residues in the extracellular loop of β4 subunits that are important for Vt3.1 inhibition of the channel (Fig. 4).

To understand how Vt3.1 inhibits the channel, we modeled the structure of Vt3.1 (Fig. 7) using structure prediction tools and molecular dynamics simulations. Vt3.1 lacks ordered secondary structures (Fig. 7*A*), which is consistent with the previous circular dichroism analysis (17). Each single chain in the Vt3.1 dimer presents an "L" conformation, where Cys^9 of one peptide and Cys^{11} of the other peptide form cross-intermolecular disulfides. The two flexible N termini exhibit positive electric potentials and are close to each other, forming a positively charged and flexible domain (Fig. 7*B*). A perspective of the structures of Vt3.1 and the Kv1.2 K^+ channel (23) is shown (Fig. 7*C*). Comparing to Kv1.2, the slo1 subunit of BK channels has an additional S0 transmembrane segment (24); the positions of transmembrane segments of mslo1 and β4 were mapped based on disulfide cross-linking studies (25) (Fig. 7*D*). The extracellular loop of the BK channel β subunits extends to the central pore based on previous biophysical and pharmacological studies (26, 27), but it is not known how the loop relates to other parts of slo1. Our results suggest that the acidic residues in the β4 extracellular loop may be located close to the N terminus, the S1–S2 and S5–P linkers, because they all interact with the positive charges in Vt3.1 (Figs. 4, 5, and 7*D*). Taken together, our results suggest that the interactions between Vt3.1 and the mslo1/β4 channel may alter voltage sensor movements or the coupling between voltage sensors and the pore to reduce voltage-dependent activation of the channel.

DISCUSSION

Vt3.1 belongs to a novel class of conopeptides (17). Our results show that Vt3.1 inhibits BK channels preferentially in the presence of the β4 subunit (Figs. 1, 2, and 4), which is the most abundant BK channel β subunit in brain (9, 10). Overall, Vt3.1 inhibits the currents by a maximum of 71% at +80 mV, where the *G-V* is saturated (Fig. 3*C*) and shifts the *G-V* relation by 45 mV at approximately half-saturation concentrations. Therefore, the toxin has two effects on channel gating: to decrease the maximum open probability and to shift the *G-V* relation to more positive voltages (Fig. 1*D*), and both effects result in a reduction of the current. At physiological conditions, the peak of neuronal action potentials has a voltage of approximately +30 mV, where the two effects of the toxin will accumulatively decrease the BK current amplitude by more than 90%. These results indicate that the toxin has a clear and strong effect on channel gating and can have a significant effect on neuronal excitability. A previous study showed that injecting Vt3.1 into mouse brain induced hyperactive behavior (17). The mechanism of this behavioral change by Vt3.1 is not known, but the effects of Vt3.1 on BK channels suggest that an inhibition of BK channels may play a role. Vt3.1 inhibits the channel via electrostatic interactions among the basic residues in Vt3.1 and the acidic residues in mslo1 and the β4 subunit (Figs. 4, 5, and 7).

Previous studies have identified peptide toxins that modulate BK channels from venoms of various animals including scorpion (28–30), cone snail (31), snake (32), bee (33), and spider (34). Among these toxins, charybdotoxin (ChTx) and iberiotoxin (IbTx) have been intensively studied for molecular pharmacology and used as an effective tool to identify BK channels in various tissues that contributed greatly in the understanding

of physiological processes and the roles of BK channels. ChTx and IbTx bind to the extracellular vestibule of slo1 and block the ionic flux through the channel (35, 36). Their binding to the channel is altered by the association of β subunits; β1 enhances the binding affinity of ChTx (37) but reduces the sensitivity of the current to IbTx (38), whereas β2 and β4 reduce sensitivity to ChTx and IbTx inhibition (8, 26). Experimental evidence suggests that these effects are mediated by the extracellular loop of the β subunits that extends to the extracellular vestibule of the pore (26, 37, 39). Similar to ChTx and IbTx, β4 reduced inhibition by slotoxin (40). Martentoxin, on the other hand, showed a more complex behavior such that it enhanced currents of BK channels in association with the β1 or β4 subunit in the presence of high (20 μM) intracellular Ca^{2+} currents while inhibiting the channel with the β4 subunit in the presence of low (10–500 nM) Ca^{2+} (41, 42). Because β4 is the major BK channel β subunit in brain, these properties render the existing toxins ineffective as a tool in studying BK channels in neuroscience. On the other hand, Vt3.1 preferentially inhibits BK channels with the association of the β4 subunit. In addition, Vt3.1 acts on BK channels fast, and the effects can be readily washed out (Fig. 2); it is formed by small peptides and easy to synthesize. All these characteristics make Vt3.1 an ideal tool uniquely suited in neuroscience involving BK channels.

Unlike previously studied BK channel inhibitory peptide toxins, Vt3.1 modulates voltage-dependent gating instead of blocking the pore of BK channels (Fig. 3). By studying the mechanism of Vt3.1 inhibition of mslo1 + β4 channels, we show that Vt3.1 can be used as an effective tool to probe the structure and function of these channels. Multiple acidic amino acids in the extracellular linkers between membrane spanning helices in slo1 (Fig. 5) and the extracellular loop of β4 (Fig. 4) contribute to the inhibitory effects of Vt3.1, suggesting a large interaction interface between the slo1 and β4, as well as a large interaction interface between Vt3.1 and the channel. Interestingly, the structural model of Vt3.1 (Fig. 7, *A* and *B*) fits nicely to the structural model of mslo1 + β4 (Fig. 7, *C* and *D*), with the positive charges in Vt3.1 tracing acidic residues in the channel protein. This mode of interaction is consistent with the functional data (Fig. 3), and together these results suggest that Vt3.1 inhibits voltage sensor movements or the coupling between the voltage sensor and the pore, or both, to inhibit voltage-dependent activation. It has been shown that the association of the β1, β2, and β4 subunit alters voltage sensor movements of slo1 (43), and the extracellular loop of the β1 subunit contributes to such modulations (44). The alteration of the β4 subunit extracellular loop by Vt3.1 alters voltage-dependent activation, indicating that the extracellular loop also contributes to the β4 modulation of mslo1 voltage-dependent gating mechanism.

BK channels shorten action potentials and contribute to the fast after hyperpolarization in neurons (1), thereby regulating neuronal firing frequency (2) and synaptic transmission (3). Aberrant BK channel function may lead to neurological diseases. A mutation in human slo1 that enhances BK channel Ca^{2+} sensitivity has been associated with epilepsy and paroxysmal dyskinesia (45, 46). Consistently, knockout of the BK channel β4 subunit, which enhanced BK channel activity, resulted in seizure in mouse (47). Recently, it has been shown that the fragile X mental retardation protein (FMRP) regulates presynaptic activity by interacting with the β4 subunit and modulating BK channel function (48). Therefore, drugs that modulate neuronal BK channels may provide therapy for BK channel-associated neurological diseases. Our results demonstrate that BK channel with β4 subunits can be specifically targeted by a compound (Fig. 1) that interacts with the acidic residues in the extracellular loop of β4 (Fig. 4) to modulate channel function.

Acknowledgments—The mslo1 and β subunits clone were kindly provided by Drs. Lawrence Salkoff, Chris Lingle (Washington University), and Robert Brenner (University of Texas Health Science Center at San Antonio). We thank Drs. Urvi Lee, Junqiu Yang, and Xiaohui Sun and Mark Zaydman for helpful suggestions on experiments and data analyses.

REFERENCES

1. Lancaster, B., and Nicoll, R. A. (1987) Properties of two calcium-activated hyperpolarizations in rat hippocampal neurones. *J. Physiol.* **389,** 187–203
2. Gu, N., Vervaeke, K., and Storm, J. F. (2007) BK potassium channels facilitate high-frequency firing and cause early spike frequency adaptation in rat CA1 hippocampal pyramidal cells. *J. Physiol.* **580,** 859–882
3. Robitaille, R., and Charlton, M. (1992) Presynaptic calcium signals and transmitter release are modulated by calcium-activated potassium channels. *J. Neurosci.* **12,** 297–305
4. Meredith, A. L., Wiler, S. W., Miller, B. H., Takahashi, J. S., Fodor, A. A., Ruby, N. F., and Aldrich, R. W. (2006) BK calcium-activated potassium channels regulate circadian behavioral rhythms and pacemaker output. *Nat. Neurosci.* **9,** 1041–1049
5. Brayden, J., and Nelson, M. (1992) Regulation of arterial tone by activation of calcium-dependent potassium channels. *Science* **256,** 532–535
6. Cui, J., Yang, H., and Lee, U. S. (2009) Molecular mechanisms of BK channel activation. *Cell. Mol. Life Sci.* **66,** 852–875
7. McManus, O. B., Helms, L. M., Pallanck, L., Ganetzky, B., Swanson, R., and Leonard, R. J. (1995) Functional role of the β subunit of high conductance calcium-activated potassium channels. *Neuron* **14,** 645–650
8. Wallner, M., Meera, P., and Toro, L. (1999) Molecular basis of fast inactivation in voltage and Ca^{2+}-activated K^+ channels: A transmembrane β-subunit homolog. *Proc. Natl. Acad. Sci. U.S.A.* **96,** 4137–4142
9. Brenner, R., Jegla, T. J., Wickenden, A., Liu, Y., and Aldrich, R. W. (2000) Cloning and functional characterization of novel large conductance calcium-activated potassium channel beta subunits, hKCNMB3 and hKCNMB4. *J. Biol. Chem.* **275,** 6453–6461
10. Weiger, T. M., Holmqvist, M. H., Levitan, I. B., Clark, F. T., Sprague, S., Huang, W.-J., Ge, P., Wang, C., Lawson, D., Jurman, M. E., Glucksmann, M. A., Silos-Santiago, I., DiStefano, P. S., and Curtis, R. (2000) A novel nervous system β subunit that downregulates human large conductance calcium-dependent potassium channels. *J. Neurosci.* **20,** 3563–3570
11. Terlau, H., and Olivera, B. M. (2004) *Conus* venoms. A rich source of novel ion channel-targeted peptides. *Physiol. Rev.* **84,** 41–68
12. Olivera, B. M. (2006) *Conus* peptides. Biodiversity-based discovery and exogenomics. *J. Biol. Chem.* **281,** 31173–31177
13. Lewis, R. J., Dutertre, S., Vetter, I., and Christie, M. J. (2012) *Conus* venom peptide pharmacology. *Pharmacol. Rev.* **64,** 259–298
14. Bowersox, S. S., and Luther, R. (1998) Pharmacotherapeutic potential of omega-conotoxin MVIIA (SNX-111), an N-type neuronal calcium channel blocker found in the venom of *Conus magus*. *Toxicon* **36,** 1651–1658
15. Duray, H. P., Hatfill, J. S., and Pellis, R. N. (1997) Venom peptides as human pharmaceuticals. *Sci. Med.* **4,** 6
16. Miljanich, G. P. (2004) Ziconotide. Neuronal calcium channel blocker for treating severe chronic pain. *Curr. Med. Chem.* **11,** 3029–3040
17. Wu, X. C., Zhou, M., Peng, C., Shao, X. X., Guo, Z. Y., and Chi, C. W. (2010) Novel conopeptides in a form of disulfide-crosslinked dimer. *Peptides* **31,** 1001–1006

18. Lee, U. S., and Cui, J. (2009) β subunit-specific modulations of BK channel function by a mutation associated with epilepsy and dyskinesia. *J. Physiol.* **587,** 1481–1498
19. Butler, A., Tsunoda, S., McCobb, D. P., Wei, A., and Salkoff, L. (1993) mSlo, a complex mouse gene encoding "maxi" calcium-activated potassium channels. *Science* **261,** 221–224
20. Shi, J., Krishnamoorthy, G., Yang, Y., Hu, L., Chaturvedi, N., Harilal, D., Qin, J., and Cui, J. (2002) Mechanism of magnesium activation of calcium-activated potassium channels. *Nature* **418,** 876–880
21. Maupetit, J., Derreumaux, P., and Tuffery, P. (2009) PEP-FOLD. An online resource for de novo peptide structure prediction. *Nucleic Acids Res.* **37,** W498–W503
22. Phillips, J. C., Braun, R., Wang, W., Gumbart, J., Tajkhorshid, E., Villa, E., Chipot, C., Skeel, R. D., Kalé, L., and Schulten, K. (2005) Scalable molecular dynamics with NAMD. *J. Comput. Chem.* **26,** 1781–1802
23. Long, S. B., Campbell, E. B., and Mackinnon, R. (2005) Crystal structure of a mammalian voltage-dependent Shaker family K^+ channel. *Science* **309,** 897–903
24. Meera, P., Wallner, M., Song, M., and Toro, L. (1997) Large conductance voltage- and calcium-dependent K^+ channel, a distinct member of voltage-dependent ion channels with seven N-terminal transmembrane segments (S0-S6), an extracellular N terminus, and an intracellular (S9–S10) C terminus. *Proc. Natl. Acad. Sci. U.S.A.* **94,** 14066–14071
25. Liu, G., Niu, X., Wu, R. S., Chudasama, N., Yao, Y., Jin, X., Weinberg, R., Zakharov, S. I., Motoike, H., Marx, S. O., and Karlin, A. (2010) Location of modulatory β subunits in BK potassium channels. *J. Gen. Physiol.* **135,** 449–459
26. Meera, P., Wallner, M., and Toro, L. (2000) A neuronal β subunit (KCNMB4) makes the large conductance, voltage- and Ca^{2+}-activated K^+ channel resistant to charybdotoxin and iberiotoxin. *Proc. Natl. Acad. Sci. U.S.A.* **97,** 5562–5567
27. Zeng, X. H., Xia, X. M., and Lingle, C. J. (2003) Redox-sensitive extracellular gates formed by auxiliary [beta] subunits of calcium-activated potassium channels. *Nat. Struct. Biol.* **10,** 448–454
28. Miller, C., Moczydlowski, E., Latorre, R., and Phillips, M. (1985) Charybdotoxin, a protein inhibitor of single Ca^{2+}-activated K^+ channels from mammalian skeletal muscle. *Nature* **313,** 316–318
29. Galvez, A., Gimenez-Gallego, G., Reuben, J. P., Roy-Contancin, L., Feigenbaum, P., Kaczorowski, G. J., and Garcia, M. L. (1990) Purification and characterization of a unique, potent, peptidyl probe for the high conductance calcium-activated potassium channel from venom of the scorpion *Buthus tamulus*. *J. Biol. Chem.* **265,** 11083–11090
30. Yao, J., Chen, X., Li, H., Zhou, Y., Yao, L., Wu, G., Chen, X., Zhang, N., Zhou, Z., Xu, T., Wu, H., and Ding, J. (2005) BmP09, a "long chain" scorpion peptide blocker of BK channels. *J. Biol. Chem.* **280,** 14819–14828
31. Fan, C., Chen, X. K., Zhang, C., Wang, L. X., Duan, K.-L., He, L.-L., Cao, Y., Liu, S.-Y., Zhong, M.-N., Ulens, C., Tytgat, J., Chen, J.-S., Chi, C.-W., and Zhou, Z. (2003) A novel conotoxin from *Conus betulinus*, κ-BtX, unique in cysteine pattern and in function as a specific BK channel modulator. *J. Biol. Chem.* **278,** 12624–12633
32. Wang, J., Shen, B., Guo, M., Lou, X., Duan, Y., Cheng, X. P., Teng, M., Niu, L., Liu, Q., Huang, Q., and Hao, Q. (2005) Blocking effect and crystal structure of natrin toxin, a cysteine-rich secretory protein from *Naja atra* venom that targets the BKCa channel. *Biochemistry* **44,** 10145–10152
33. Kanjhan, R., Coulson, E. J., Adams, D. J., and Bellingham, M. C. (2005) Tertiapin-Q blocks recombinant and native large conductance K^+ channels in a use-dependent manner. *J. Pharmacol. Exp. Ther.* **314,** 1353–1361
34. Windley, M. J., Escoubas, P., Valenzuela, S. M., and Nicholson, G. M. (2011) A novel family of insect-selective peptide neurotoxins targeting insect large-conductance calcium-activated K^+ channels isolated from the venom of the theraphosid spider *Eucratoscelus constrictus*. *Mol. Pharmacol.* **80,** 1–13
35. MacKinnon, R., and Miller, C. (1988) Mechanism of charybdotoxin block of the high-conductance, Ca^{2+}-activated K^+ channel. *J. Gen. Physiol.* **91,** 335–349
36. Giangiacomo, K. M., Garcia, M. L., and McManus, O. B. (1992) Mechanism of iberiotoxin block of the large-conductance calcium-activated potassium channel from bovine aortic smooth muscle. *Biochemistry* **31,** 6719–6727
37. Hanner, M., Schmalhofer, W. A., Munujos, P., Knaus, H.-G., Kaczorowski, G. J., and Garcia, M. L. (1997) The β subunit of the high-conductance calcium-activated potassium channel contributes to the high-affinity receptor for charybdotoxin. *Proc. Natl. Acad. Sci. U.S.A.* **94,** 2853–2858
38. Dworetzky, S. I., Boissard, C. G., Lum-Ragan, J. T., McKay, M. C., Post-Munson, D. J., Trojnacki, J. T., Chang, C.-P., and Gribkoff, V. K. (1996) Phenotypic alteration of a human BK (hSlo) channel by hSloβ subunit coexpression. Changes in blocker sensitivity, activation/relaxation and inactivation kinetics, and protein kinase A modulation. *J. Neurosci.* **16,** 4543–4550
39. Xia, X. M., Ding, J. P., and Lingle, C. J. (1999) Molecular basis for the inactivation of Ca^{2+}- and voltage-dependent BK channels in adrenal chromaffin cells and rat insulinoma tumor cells. *J. Neurosci.* **19,** 5255–5264
40. Garcia-Valdes, J., Zamudio, F. Z., Toro, L., and Possani, L. D. (2001) Slotoxin, αKTx1.11, a new scorpion peptide blocker of MaxiK channels that differentiates between α and α+β (β1 or β4) complexes. *FEBS Lett.* **505,** 369–373
41. Shi, J., He, H. Q., Zhao, R., Duan, Y.-H., Chen, J., Chen, Y., Yang, J., Zhang, J. W., Shu, X. Q., Zheng, P., and Ji, Y. H. (2008) Inhibition of martentoxin on neuronal BK channel subtype (α+β4). Implications for a novel interaction model. *Biophys. J.* **94,** 3706–3713
42. Tao, J., Shi, J., Yan, L., Chen, Y., Duan, Y. H., Ye, P., Feng, Q., Zhang, J. W., Shu, X. Q., and Ji, Y. H. (2011) Enhancement effects of martentoxin on glioma BK channel and BK channel (α+β1) subtypes. *PLoS One* **6,** e15896
43. Contreras, G. F., Neely, A., Alvarez, O., Gonzalez, C., and Latorre, R. (2012) Modulation of BK channel voltage gating by different auxiliary β subunits. *Proc. Natl. Acad. Sci. U.S.A.* **109,** 18991–18996
44. Gruslova, A., Semenov, I., and Wang, B. (2012) An extracellular domain of the accessory β1 subunit is required for modulating BK channel voltage sensor and gate. *J. Gen. Physiol.* **139,** 57–67
45. Du, W. (2005) Calcium-sensitive potassium channelopathy in human epilepsy and paroxysmal movement disorder. *Nat. Genet.* **37,** 733–738
46. Yang, J., Krishnamoorthy, G., Saxena, A., Zhang, G., Shi, J., Yang, H., Delaloye, K., Sept, D., and Cui, J. (2010) An epilepsy/dyskinesia-associated mutation enhances BK channel activation by potentiating Ca^{2+} sensing. *Neuron* **66,** 871–883
47. Brenner, R., Chen, Q. H., Vilaythong, A., Toney, G. M., Noebels, J. L., and Aldrich, R. W. (2005) BK channel [beta]4 subunit reduces dentate gyrus excitability and protects against temporal lobe seizures. *Nat. Neurosci.* **8,** 1752–1759
48. Deng, P. Y., Rotman, Z., Blundon, J. A., Cho, Y., Cui, J., Cavalli, V., Zakharenko, S. S., and Klyachko, V. A. (2013) FMRP regulates neurotransmitter release and synaptic information transmission by modulating action potential duration via BK channels. *Neuron* **77,** 696–711
49. Vanommeslaeghe, K., Hatcher, E., Acharya, C., Kundu, S., Zhong, S., Shim, J., Darian, E., Guvench, O., Lopes, P., Vorobyov, I., and Mackerell, A. D., Jr. (2010) CHARMM General Force Field: A Force Field for Drug-Like Molecules Compatible with the CHARMM All-Atom Additive Biological Force Fields. *J. Comput. Chem.* **31,** 671–690
50. Ryckaert, J.-P., Ciccotti, G., and Berendsen, H.J.C. (1977) Numerical integration of the cartesian equations of motion of a system with constraints: molecular dynamics of n-alkanes. *J. Comput. Phys.* **23,** 327–341
51. Darden, T., York, D., and Pedersen, L. (1993) Particle mesh Ewald: An N · log(N) method for Ewald sums in large systems. *J. Chem. Phys.* **98,** 10089–10092